

Aliasing in Modal Parameter Estimation

An Historical Look and New Innovations

Håvard Vold, Kevin Napolitano and Dan Hensley, ATA Engineering, Inc., San Diego, California

Mark Richardson, Vibrant Technology, Inc., Scotts Valley, California

Experimentalists are familiar with the aliasing that happens in data acquisition when the sampling rate is less than twice the highest frequency of energy in the signal to be sampled. Much effort has been made using a combination of analog and digital filters to make sure that the higher frequencies are filtered out to avoid or minimize the effect of this aliasing. Much less talked about is the aliasing that occurs in modal parameter estimation, or curve-fitting, when the residual effects of out-of-band modes violate assumptions of the finite dimensional parametric model that the experimentalist uses to curve-fit the acquired digitized data. While the out-of-band energy has been filtered out of the now band-limited data, the tails, sometimes called residual flexibility and inertial restraint of the out of band modes, are still present in the data. This article looks at some classes of modal parameter estimation algorithms and shows by theory and example that the algorithms based on continuous time or Laplace domain formulations are superior to the discrete time domain or z domain models in that they give results that are not contaminated by the aliasing effect of these residuals.

Practitioners of the art and science of modal testing and experimental modal parameter estimation carefully choose algorithms and excitation methods for each testing situation with a balanced combination of prejudice, experience and folklore. Two popular methods in use today are narrow-band frequency domain methods using polynomials for highly damped structures, and the discrete time-complex exponential method with multiple references for high modal density and multipoint excitation. Mythologies exist on the merits of frequency domain versus time domain modal parameter estimation methods, and religious wars have been less fervent than some of the debates within the modal testing community.

The classical method of modal testing has been the tuned sine-dwell method, implemented in the middle of the last century with analog instrumentation. (Hence the nomenclature unique to ancient sine dwellers of the California desert, which is used when its proponents are out of earshot.) While there is much to be said for the advantages of exercising modes in their normal form one at a time and at high force levels, and the possibility of using damping models other than the customary linear viscous damping model, we shall limit ourselves in this article to the uses of broadband testing and curve-fitting methods due to the ease, efficiency and economy of their deployment.

Computational Modes

The motivation for this article is the pervasive existence of computational modes around the broadband modal parameter estimation methods. Such computational modes, or poles or roots, are the by-product of specifying a model order higher than the actual physical number of modes in the analysis band. It is almost always necessary to specify a model order that is "too high" in order to ensure proper identification of modes that correspond to the physical ones. The role of the extra computational modes is to fill in the cracks caused by residual effects, nonlinearities, noise and inconsistency due to mass loading, nonstationarities and a few other culprits. Since we are interested in the modal parameters of

the physical modes and not in the graphical nature of the curve fit itself, there is a fine line between choosing a model order that is too high and one that is too low. In any case, after the analysis run, the analyst is still faced with the triage of choosing those modes that clearly correspond to physical phenomena. Those that look improbable are discarded as computational modes, and those that merely look dubious are slated for closer scrutiny.

The criteria for being a computational mode include negative or improbable damping, a frequency that is outside the analysis band, or lack of persistence as modal parameters are tracked from one model order to the next. This persistence is often depicted in a variety of stability diagrams. It is clear from the diagram that certain modes are constantly found in order of progressively larger orders. A mode that traces a straight line across the stability diagram is said to be stable and is therefore assumed to represent a genuine physical mode. Parameter estimation methods with the same nominal performance may be judged quite differently in their performance when equipped with different triage criteria and stability graphics. The phenomenon that separates the continuous time methods from the discrete time methods is the nonlinear aliasing of the computational modes. The latter methods tend to put their computational modes inside the analysis band and also require more computational modes to fill in the cracks in the nonlinear data.

A Useful Dichotomy

We shall begin our investigation of computational modes by first answering the question, What is the difference between time domain and frequency domain in modal parameter estimation? The answer that we proffer – The real difference is between continuous time and discrete time. The frequency domain enthusiast should distinguish between the Laplace transform domain (continuous time) and z transform domain (discrete time). An unqualified use of the terms time domain and frequency domain is orthogonal to the pertinent characteristics of broadband modal parameter estimation. The phenomenon that most clearly divides the continuous time and the discrete time formulations is that of aliasing of computational modes as the curve fitter attempts to handle out-of-band residual effects. Low-pass filtering knocks the out-of-band resonance peaks out of the picture, while no amount of filtering will remove the residuals, tails and foothills of the out-of-band modes. In the discrete-time methods, all modal frequencies are mapped onto the analysis band, while in the continuous-time formulation, computational modes, or out-of-band phenomena, are allowed to go where they should

In practical terms, computational modes in the discrete-time methods are forced back into the analysis band, and there are also more computational modes, because this aliasing is a non linear effect that confuses linear estimation assumptions (see Figure 1). Continuous-time methods do not suffer from this weakness. The weakness of the continuous-time formulations is that of numerical ill conditioning, which rears its ugly head for larger sets of modes within an analysis band. This is cured by a change of basis of the transfer function expressions from power polynomials into some classes of orthogonal polynomials, but such methods have not achieved mainstream status yet. In this article, we look at a variety of representative continuous-time and discrete-time modal parameter estimation algorithms, look at their mathematical derivations,

Based on a paper presented at IMAC XXV, the 25th International Modal Analysis Conference, Orlando, FL, February 2007.

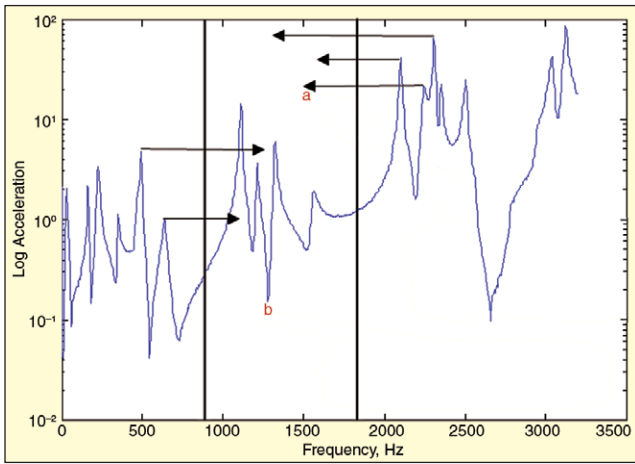


Figure 1. The mechanics of modal aliasing.

and apply them to a common analytical data set with high modal density and a plethora of residual effects. We will then summarize the behavior of the different methods with respect to the placement and characteristics of computational modes, especially with respect to aliasing of said modes.

Models

We shall consider the simplest of multifunction situations, where we have a column of the frequency response function (FRF) matrix corresponding to a single point of excitation and multiple acceleration response locations. We will also assume that a frequency band of interest has been selected, that the center frequency of this band has been translated to DC (zero radians/second), and that scaling has taken place so that the highest and lowest frequencies are $\pm\pi$ radians/second. (Typically done by a combination of zoom, low pass filtering and decimation.) The corresponding time histories of these FRF's are now complex, with time steps of one second. We select an analysis frequency band where we have strong out-of-band modes on either side. The data are from an aerospace structure that was excited with burst random excitation and with enough attenuation between bursts so that the estimated frequency response functions would be reasonably clean and leak free. Our selection of models is governed by trying to capture the behavior and characteristics of the most popular methods in use today. While most of these methods have a direct extension to multiple inputs, we shall only look at the single-input, multiple-output situation.

Direct Estimation in the Laplace and z Domains

The direct parameter frequency domain estimation methods were pioneered by people who wrote the basic equations and saw that when inputs and outputs were measured at a set of discrete frequencies, the system matrices occurred in a linear fashion. Given enough measurements, the curve-fitting equations became a set of over-determined linear equations. The model order is small, but the size of the matrices could become large. For earlier material, see References 1, 2, 3, and 4. The curve-fitting model for both a z transform and a Laplace transform formulation is a rational vector function in the transform variable; that is:

$$H(i\omega_k) = \begin{cases} A_z(z_k)^{-1}B_z(z_k), & \text{where } z_k = \exp(i\omega_k), \text{ } z \text{ domain} \\ A_L(\omega_k)^{-1}B_L(\omega_k), & \text{Laplace domain} \end{cases} \quad (1)$$

Where $\{\omega_k\}$ is the finite set of frequencies for which frequency response function data are available, and the matrix polynomials $A_*(.)$ and $B_*(.)$ are of the first order, meaning that the number of response coordinates must be at least as large as the number of effective modes in the analysis band. The highest order term of $A_*(.)$ is set to the identity matrix, and we then can write the basic equation in the z domain as:

$$A_z(z_k)H(i\omega_k) = B_z(z_k) \quad (2)$$

which after expansion of polynomial terms becomes:

$$(z_k I + A_{z0})H(i\omega_k) = B_{z1} + z_k B_{z0} \quad (3)$$

Finally, chasing the unknowns to the left side and using all the available data, Eq. 3 becomes:

$$\begin{bmatrix} A_{z0} & B_{z1} & B_{z0} \end{bmatrix} \begin{bmatrix} H(i\omega_k) \\ 1 \\ z_k \end{bmatrix} = - \begin{bmatrix} z_k H(i\omega_k) \\ z_k \end{bmatrix} \quad (4)$$

This can then be solved by some least-squares scheme for the unknowns, and we then find the z domain roots or poles as the eigenvalues of $(zI + A_{z0})v = 0$. The Laplace domain poles are then calculated as $\ln(z)$, from which viscous damping and resonance frequency are extracted. Because of the periodicity of the complex exponential $\exp(i(\omega + 2\pi)) = \exp(i\omega)$, the computed frequencies must all be contained within the analysis band $[-\pi, \pi]$. The Laplace domain equations are done in exactly the same fashion, except that the Laplace domain roots are obtained directly from the eigenvalue problem and are in no way restricted to the analysis band. *This is a key difference between the discrete- and continuous-time methods.*

Ibrahim Time Domain

The Ibrahim time domain method (ITD) was first published by Sam Ibrahim, who noted that the free decay of a vector of accelerations was governed by a constant transfer matrix. By estimating the transfer matrix, the modal parameters could be extracted.^{5,6} The control engineers entered the fray in the middle '80s and defined an equivalent method derived from a state space formulation and called it the eigenvalue realization method or, ERA.⁷ The authors added bells and whistles to allow for simultaneous incoherent multipoint excitation, so that close and repeated poles could be reliably determined. The free decay of a structure in continuous time can be expressed as:

$$X(t) = V \exp(\Lambda t) V^{-1} X(0) \quad (5)$$

where V is the matrix of eigenvectors, Λ is the diagonal matrix of Laplace domain poles. If we assume that we have data at time steps of one second apart, we then have the following decay relation between the responses one second apart:

$$X(n) = V \exp(\Lambda) V^{-1} X(n-1) \quad (6)$$

so setting $T = V \exp(\Lambda) V^{-1}$,

$$T[X(1) \dots X(k) \dots] = [X(2) \dots X(k+1) \dots] \quad (7)$$

We can find a least-squares solution for T , and then get the system poles by solving for the eigenvalues of T . Since we must take the natural logarithm of the eigenvalues of the transfer matrix T to obtain the poles, ITD is also a z domain or discrete time method. Again, the computed frequencies are restrained to the analysis band $[-\pi, \pi]$. When the ITD method is used with free decay data obtained by inverse Fourier transforms of frequency response functions, it is sometimes of interest to weight the different frequency bands according to their coherence. It is much more important, though, to discard the first few time samples, since these are not free decays, but are contaminated by the numerator terms in the rational transfer function. To see this, we take the inverse Fourier transform of the z domain transfer function $H(z)$ in Eq. 1, which results in a convolution expression for the unit impulse response $H(n)$ in discrete time as:

$$\sum_{k=0}^N A_{zk} h(n-k) = \sum_{k=0}^M b_{zk} \delta(n-k) \quad (8)$$

where $\delta(.)$ is the Dirac delta and N and M are the number of terms in the denominator and numerator matrix polynomials. While this defines the unit impulse response, the algorithms formulated in terms of free decay must have shed any excitation function before the measurements are usable in these algorithms. Then we rewrite Eq. 8 as:

$$\sum_{k=0}^N A_{zk} h(n-k) = \begin{cases} B_{zn}, & 0 \leq n \leq M \\ 0, & n < 0 \text{ or } n > M \end{cases} \quad (9)$$

For the case where we have more functions than the effective number of modes, $N = M + 1$, and we see from Eq. 9 that we must skip at least the first two samples from the unit impulse response.

This is also indicated in Eq. 7.

Complex Exponential

The complex exponential method was first used with real exponentials; that is, only decay terms back in 1795.⁸ Later, in the 1950s, it found use as a vibration tool with complex exponentials.⁹ In the early '80s, one of the authors used this method as the basis for a method that exploited multiple references, or exciter locations, to enable the estimation of closely coupled modes and repeated roots.^{10,11,12} This method was named 'polyreference' and has become perhaps the dominant method in commercial use today. Here we restrict ourselves to a single reference that handles the sample data set. The main difference between the complex exponential method and the ITD method is that the latter is a low-order method, while the former looks at one response coordinate at a time and thus becomes a high-order method. Let us now look at the individual unit-impulse response functions of the measured channels, rewriting Eq. 9 in scalar form and letting the subscript z denote a generic channel:

$$\sum_{k=0}^N a_k h_z(n-k) = \begin{cases} b_{zn}, & 0 \leq n \leq M \\ 0, & n < 0 \text{ or } n > M \end{cases} \quad (10)$$

Frequency weighting before applying the inverse Fourier transform is optional and seldom called for. Since the resonances of a structure are assumed to be global entities, we are free to use a common-denominator polynomial:

$$a(z) = \sum_{k=0}^N z^{N-k} a_k \quad (11)$$

The numerator polynomials are location dependent and define the mode shape coefficients or residues at the corresponding measurement locations. Again, we let $N = M =$ number of effective modes in the analysis interval. Just as in the ITD method, we need to discard the first $M + 1$ samples of the unit impulse response to reach the free-decay position. Now, normalizing the leading coefficient to unity so that we have a monic denominator polynomial, we can use the discrete unit impulse response functions to write an overdetermined equation set for this polynomial:

$$aT_z \approx 0 \quad (12)$$

where:

$$a = [1 \ a_1 \ \dots \ a_k \ \dots \ a_N], \text{ and}$$

and

$$T_z = \begin{pmatrix} h_z(N+M+1) & \dots & h_z(N+M+1+n) \\ \vdots & \dots & \vdots \\ h_z(N+M+1-k) & \dots & h_z(N+M+1+1) \\ \vdots & \dots & \vdots \\ h_z(M+1) & \dots & h_z(M+1+n) \end{pmatrix} \quad (13)$$

We keep adding columns until the first time history in T_z goes end around. By inspecting the structure of Eq. 13, one can see that the rows of T_z are time-shifted sections of the unit impulse response function $h_z(n)$, defining the row vector:

$$\tilde{h}_z(p,q) = [h_z(p+1) \ \dots \ h_z(p+n) \ \dots \ h_z(p+1+q)] \quad (14)$$

the data matrix of Eq. 13 can also be written as:

$$T_z = \begin{pmatrix} \tilde{h}_z(M+N,\dots) \\ \vdots \\ \tilde{h}_z(M+N-k,\dots) \\ \vdots \\ \tilde{h}_z(M,\dots) \end{pmatrix} \quad (15)$$

Since the scalar denominator polynomial is the same for all response channels, we can rewrite Eq. 12 using all the responses as the overdetermined system of equations:

$$a[T_1 \ T_2 \ \dots \ T_k \ \dots \ T_N] \approx 0 \quad (16)$$

where N is the number of frequency response functions. A least-squares solution through normal equations may be had by solving

the positive semidefinite hermitian equations:

$$a([T_1 \ T_2 \ \dots \ T_k \ \dots \ T_N][T_1 \ T_2 \ \dots \ T_k \ \dots \ T_N]^H) = 0 \quad (17)$$

which can be written as:

$$aT = 0, \text{ where } T = \sum_{n=1}^N T_n T_n^H \quad (18)$$

The polynomial a is normally found by normalizing the leading coefficient to one and solving Eq. 18. The poles of this system will then be the natural logarithm of the roots of Eq. 11, and the frequencies are kept within the analysis band. This leads to the possible aliasing of the computational modes. Looking at Eq. 10, we can easily calculate the numerator polynomials for residue determinations once the denominator polynomial is known.

Least-Squares Complex Frequency Domain

At the turn of the millennium, a series of papers on a new z domain modal parameter estimation method came out of the milieus at the Free University in Brussels and the software house LMS International.^{13,14,15,16} The motivation was to construct a method that would be easier to use and lead more directly to a complete and valid modal model from a set of frequency response function measurements from one or more exciter locations. This method is also referred to as just LSCF. (Since we have no access to the internals of the commercial implementations, this article is based solely on the published body of work pertaining to the LSCF method.) For the purpose of this article, we will also restrict this method to the case of a single-force input location and multiple of response locations. The basic equation for this scheme is to write the scalar form of Eq. 1 in the z domain for the channel z :

$$H_z(i\omega_k) = \frac{b_z(z_k)}{a_z(z_k)}, z_k = \exp(i\omega_k) \quad (19)$$

Multiplying out the denominator polynomial, Eq. 19 becomes:

$$a(z_k)H_z(i\omega_k) = b_z(z_k) \quad (20)$$

Here we see that the unknown polynomial coefficients appear in a linear fashion and are amenable to least-squares estimation. We next express Eq. 20 explicitly with the error term ϵ_k using the numerator and denominator polynomial coefficients, including all $K + 1$ frequency lines, rearrange and obtain:

$$[b \ a] \begin{bmatrix} X \\ Y_z \end{bmatrix} = \epsilon_z \quad (21)$$

with

$$X = \begin{bmatrix} z_0^M & z_1^M & \dots & z_K^M \\ z_0^{M-1} & z_1^{M-1} & \dots & z_K^{M-1} \\ \vdots & \vdots & \ddots & \vdots \\ z_0^0 & z_1^0 & \dots & z_K^0 \end{bmatrix} \quad (22)$$

and

$$Y_z = \begin{bmatrix} z_0^N H(i\omega_0) & z_1^N H(i\omega_1) & \dots & z_K^N H(i\omega_k) \\ z_0^{N-1} H(i\omega_0) & z_1^{N-1} H(i\omega_1) & \dots & z_K^{N-1} H(i\omega_k) \\ \vdots & \vdots & \ddots & \vdots \\ z_0^0 H(i\omega_0) & z_1^0 H(i\omega_1) & \dots & z_K^0 H(i\omega_k) \end{bmatrix} \quad (23)$$

A minimum norm solution for the denominator polynomial in is found by minimizing the quadratic form,

$$\min_{a_0=1} \|\epsilon_z\|^2 = \min_{a_0=1} [b_z \ a] \begin{bmatrix} XX^H & Y_z Y_z^H \\ XY_z^H & YY_z^H \end{bmatrix} [b_z \ a]^H \quad (24)$$

By setting $b_z = -aXY_z^H(XX^H)^{-1}$ the numerator term can be eliminated from Eq. 24, leading to the form:

$$\min_{a_0=1} \|\epsilon_z\|^2 = \min_{a_0=1} a(Y_z Y_z^H - Y_z(XX^H)^{-1}XY_z^H)a^H \quad (25)$$

Finally, a global solution is found by summing over all response channels z and minimizing the global error norm:

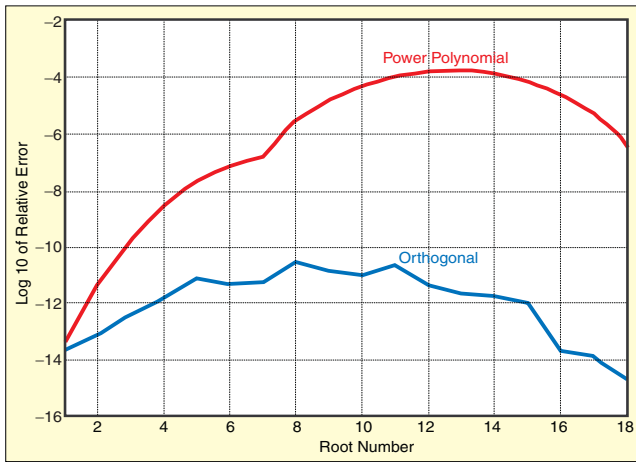


Figure 2. Numerical error in polynomial solve using power polynomials and orthogonal polynomials as basis functions.

$$\min_{a_0=1} \sum_z \|\varepsilon_z\|^2 = aT a^H, \text{ where } T = \sum_z (Y_z Y_z^H - Y_z (X X^H)^{-1} X Y_z^H) \quad (26)$$

A standard least-squares solution is obtained by minimizing Eq. 26 subject to setting the leading coefficient a_0 to unity, while a total least-squares solution is found by minimizing subject to keeping the global norm equal to unity:

$$\min_{\|a\|=1} \sum_z \|\varepsilon_z\|^2 = \min_{\|a\|=1} aT a^H \quad (27)$$

The Relationship to the Complex Exponential Method

Next we will show that the published LSCF and the complex exponential methods are essentially the same. The mathematical details are given in a following section (“The equivalence of LSCF and LSCE”). We can see from this derivation that for a single exciter location, LSCF and LSCE (the classical complex exponential method) are mathematically equivalent when no frequency domain weighting is used. It can similarly be shown that Polyreference implementations of the same two methods are mathematically equivalent. The numerical difference between the two formulations is in the application of the exceedingly benign discrete Fourier transform, which constitutes a rotation without any distortion of the least-squares formulations of the curve-fitting equations. We can also conclude from this that claiming that one method is superior to the other is not valid. The true distinction between curve-fitting methods lies in the use of continuous- versus discrete-time models. The LSCF method is the same as the LSCE method and suffers from the aliasing of computational modes, just as all other discrete domain methods. Furthermore, our experience shows that when one forgets to remove the leading elements of the unit impulse responses to reach the free-decay portions, both the LSCE and thereby the classical polyreference methods seem to sprout computational modes due to the violation of the free decay assumption.

The Laplace-domain rational fraction orthogonal polynomial method^{17,18,19} was introduced around 1975, where the authors succeeded in solving smaller models with less than 10 modes. The estimates are very clean, and specifically, the residual effects are relegated to the outside of the analysis frequency band. These methods were observed to be alias free¹⁸ due to being formulated in continuous time, a benefit of exploiting the bounded spectrum of the acquired data. Vold and students at the University of Cincinnati determined in the mid '80s that the weakness of high-order models in the Laplace domain lay in the transformation of the characteristic polynomial in an orthogonal polynomial basis back to the power polynomials before solving for the modes. This weakness was resolved by formulating the direct solution in orthogonal coordinates through a generalized companion matrix eigenvalue problem^{20,21} and a number of papers and theses written in the circles of the University of Cincinnati and SDRC. With this one change of the solution procedure, the limitation of order size went from less than 10 to as high as your patience would last, waiting

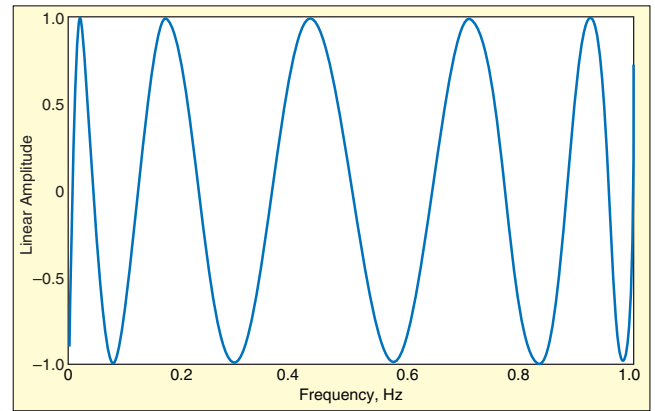


Figure 3. Orthogonal polynomial.

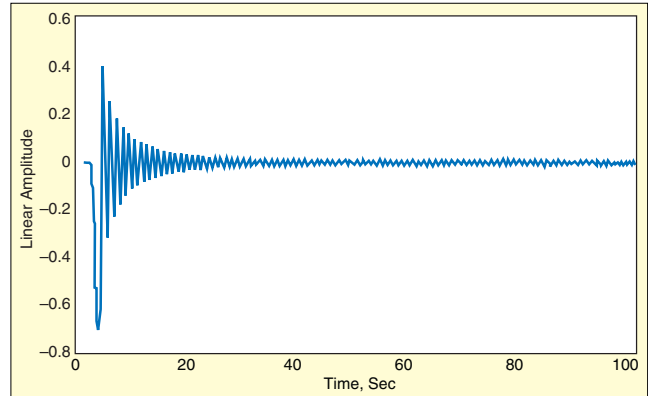


Figure 4. Green's function from orthogonal polynomial.

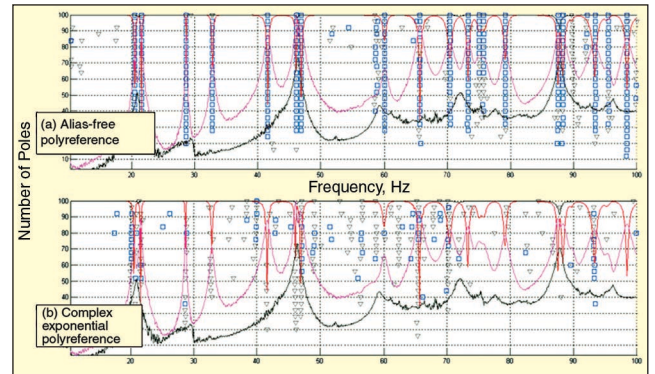


Figure 5. Alias free and aliased stability diagrams.

for the computer to finish the calculations.

Vold worked in the mid '90s with researchers at the Free University of Brussels in Belgium to introduce the use of orthogonal polynomials and the generalized companion matrix to Laplace domain system identification algorithms for controls and electrical engineering applications.^{22,23,24} In these papers, the numerical and statistical performance of the orthogonal polynomials was also formally investigated, and shown to allow for the successful and predictable performance of high-order models, something deemed impossible before in the Laplace domain or the continuous-time domain. Figure 2 shows a graphic difference in the error generated with the use of ordinary power polynomials versus orthogonal polynomials in solving for the roots of a polynomial of order 18.

AFPoly, the Alias-Free Polyreference Method

This method is based on the Laplace domain orthogonal polynomial rational fraction method, with the added use of a generalized orthogonal polynomial companion matrix that allows for the numerical stability over an entire frequency range containing hundreds and even thousands of modes. For an example of an orthogonal polynomial, see Figure 3.

The key observation is that we are working on test data that are

bounded in the frequency domain and, appealing to the sampling theorem, the formulation may be phrased in terms of continuous time or the Laplace domain. Now, the orthogonality properties of the orthogonal polynomials in the Laplace domain induces an orthogonality property of the inverse infinite Fourier transform of these polynomials in the continuous time domain. Since the orthogonal polynomials are nonzero only over the bounded frequency range of the low-pass-filtered test data, the inverse infinite Fourier transform of these polynomials, the so called Green's functions are well defined wavelets with finite energy (see Figure 4).

In the continuous time domain, the usual differential equations of motion translate into convolution integrals with these finite-energy Greens functions, and the usual numerical problems with higher-order differentials vanish. Using these convolution integrals, we can also annihilate the differential operators on the force contributions in the time domain so that meaningful instrumental variables may be defined to process response data with unmeasured broadband excitation. The size of the equation systems is minimized by considering the adjoining system, exchanging the role of excitation and response just as is done in the polyreference method.

The main advantage of this method is that the residual effects of modes outside the frequency band of analysis are kept outside this band, avoiding the nonlinear effects of aliasing. One may compare the improved clarity of an AFPoly stability diagram compared to the aliased complex exponential diagram in Figure 5.

A patent application that contains an exposition in full detail has been filed.²⁵

Equivalence of LSCF and LSCE

Proof of the equivalence of LSCF and LSCE. We first note that a unitary matrix U , satisfies $U^H U = I$ by definition. It is also true that the Euclidian norm of a vector, $\|v\|^2 = v^H v$, does not change when multiplied with a unitary matrix, since $\|Uv\|^2 = (Uv)^H Uv = v^H U^H Uv = v^H I v = \|v\|^2$. Next, we note that the matrix X defined in Eq. 22 satisfies $XX^H = (K+1)I$, since by inspection, the rows of X are the discrete Fourier transform coefficients of the transform of length $K+1$. We can then easily see that the matrix U is unitary, when:

$$U = \frac{1}{\sqrt{K+1}} \begin{bmatrix} X \\ X^\perp \end{bmatrix} = \begin{bmatrix} U_1 \\ U_2 \end{bmatrix} \quad (28)$$

where X^\perp is a unitary complement of X .

Also, when a row vector of length $K+1$ is multiplied by U^H , it is inversely discrete Fourier transformed. Noting that the unitary matrix U of Eq. 28 does not change the Euclidian norm of a vector, we see from Eq. 21 that:

$$\|\varepsilon_z\|^2 = \left\| \begin{bmatrix} b_z & a \end{bmatrix} \begin{bmatrix} X \\ Y_z \end{bmatrix} U^H \right\|^2 \quad (29)$$

so that minimizing Eq. 29 gives the same result as minimizing Eq. 24. Expanding the equation above and using Eq. 28 shows that:

$$\begin{bmatrix} b_z & a \end{bmatrix} \begin{bmatrix} X \\ Y_z \end{bmatrix} U^H = \begin{bmatrix} b_z & a \end{bmatrix} \begin{bmatrix} I & 0 \\ Y_z U_1^H & Y_z U_2^H \end{bmatrix} \quad (30)$$

and that by setting:

$$b_z = -a Y_z U_1^H \quad (31)$$

when denominator a is known allows us to write the error norm as:

$$\|\varepsilon_z\|^2 = \left\| a Y_z U_2^H \right\|^2 \quad (32)$$

To gain an understanding of Eq. 32, consider row p of Y_z , which is:

$$\left[z_0^{N-p} H_z(i\omega_0) \quad z_1^{N-p} H_z(i\omega_1) \quad \dots \quad z_k^{N-p} H_z(i\omega_k) \quad \dots \right] \quad (33)$$

Inspecting this expression shows that this is the discrete Fourier transform of $h_z(n + (N-p))$ by the basic rule for forming the Fourier transformation of a time-shifted function. Likewise, consider column q of U_2^H , which is:

$$\frac{1}{\sqrt{K+1}} \left[z_0^{-(M+1+q)} \quad z_1^{-(M+1+q)} \quad \dots \quad z_k^{-(M+1+q)} \quad \dots \right]^H \quad (34)$$

and produces time point $M+1+q$ of the inverse Fourier transform when postmultiplying a row frequency domain vector. For example, element p, q of the $Y_z U_2^H$ will be $h_z(M+1+q + (N-p)) = h_z(M+N+1+q-p)$. So Eq. 32 can be expressed as:

$$\|\varepsilon_z\|^2 = \left\| a \begin{bmatrix} h_z(M+N+1) & \dots & h_z(M+N+1+n) & \dots \\ h_z(M+N) & \dots & h_z(M+N+n) & \dots \\ \vdots & \ddots & \vdots & \ddots \\ h_z(M+1) & \dots & h_z(M+1+n) & \dots \end{bmatrix} \right\|^2 \quad (35)$$

which, using the notation of Eq. 14 and Eq. 15 can be written as:

$$\|\varepsilon_z\|^2 = \left\| a \begin{bmatrix} \tilde{h}_z(M+N, \dots) \\ \tilde{h}_z(M+N-1, \dots) \\ \vdots \\ \tilde{h}_z(M, \dots) \end{bmatrix} \right\|^2 \quad (36)$$


We therefore see from Eqs. 36, 12, 13, and 15 that for a single exciter location, LSCF and LSCE (the classical complex exponential method) are mathematically equivalent when no frequency domain weighting is used.

References

- Link, M.; Vollen, A., "Identification of Structural System Parameters from Dynamic Response Data," *Zeitschrift für Flugwissenschaften*, Vol. 2, No. 3, pp. 165-174, 1978.
- Coppolino, R. N., "A Simultaneous Frequency Domain Technique for Estimation of Modal Parameters from Measured Data," SAE Paper No. 811046, p. 12., 1981.
- Leuridan, J., "Direct System Parameter Identification of Mechanical Structures with Application to Modal Analysis," Master of Science Thesis, University of Cincinnati, 1981.
- Vold, H.; Leuridan, J., "A Generalized Frequency Domain Method for Structural Parameter Estimation," 7th Seminar on Modal Analysis, Katholieke Universiteit Leuven, Belgium, September 1982.
- Ibrahim, S. R., and Mikulcik, E. C., "A Method for the Direct Identification of Vibration Parameters from the Free Response," *The Shock and Vibration Bulletin*, 47(4):183-198, 1977.
- Ibrahim, S. R., "Random Decrement Technique for Modal identification of Structures," *Journal of Spacecraft*, 14(11):696-700, 1977.
- Juang, J.-N., and Pappa, R., "An Eigensystem Realization Algorithm Formodal Parameter Identification and Reduction," *Journal of Guidance, Control and Dynamics*, 8(5):620-627, 1985
- de Prony, Gaspard Clair Francois Marie Riche, *Essai experimental et analytique: Sur les lois de la dilatabilite des fluides elastiques et sur celles de la force expansive de la vapeur de l'eau et de la vapeur de l'alkool, a differentes temperatures*, *Journal de l'Ecole Polytechnique*, Paris, 1:24-76, 1795.
- Spitznogle, F. R., and Quazi, A. H., "Representation and Analysis Of Time-Limited Signals Using a Complex Exponential Algorithm," *Journal of the Acoustical Society of America*, 47:1150-1155, 1970.
- Vold, H., Kundrat, J., Rocklin, G. T., Russel, R., "A Multi-Input Modal Estimation Algorithm for Mini-Computers," SAE Technical Paper No. 820194, International Congress and Exposition, Detroit, Michigan, February 1982.
- Vold, H., Rocklin, G.T., "The Numerical Implementation of a Multi-Input Modal Estimation Method for Mini-Computers", International Modal Analysis Conference, Orlando, 1982.
- Vold, H., Russel, R., "Advanced Analysis Methods Improve Modal Test Results," *Sound and Vibration*, March 1983.
- Vanlanduit, S., Verboven, P., Schoukens, J., and Guillaume, P., "An Automatic Frequency Domain Modal Parameter Estimation Algorithm," Proc. Of Int. Conf on Structural System Identificazion, Kassel, Germany, pp. 637-646, 2001.
- Van der Auweraer, H., Guillaume, P., Verboven, P., and Vanlanduit, S., "Application of a Fast-Stabilizing Frequency Domain Parameter Estimation Method," *ASME Journal of Dynamic Systems, Measurement, and Control*, 123(4):651-658, 2001.
- Guillaume, P., Verboven, P., Vanlanduit, S., Van der Auweraer, H., and Peeters, B. A., "Polyreference Implementation of the Least-Squares Complex Frequency Domain Estimator," Proc. of IMAC 21, the Int. Modal Analysis Conf., Kissimmee, Florida, 2003.
- Peeters, B., Guillaume, P., Van der Auweraer, H., Cauberghe, B., Verboven, P., and Leuridan, J., "Automotive and Aerospace Applications of the Polymax Modal Parameter Estimation Method," Proc. of IMAC 22, the Int. Modal Analysis Conf., Dearborn, Michigan, 2004.
- Miramand, N., Billand, J. F., LeLeux, F., and Kernevez, J. P., "Identification of Structural Modal Parameters by Dynamic Tests at a Single Point," France.
- Formenti, D., Richardson, M., "Parameter Estimation from Frequency

- Response Measurements Using Rational Fraction Polynomials," Proceedings of the 1st International Modal Analysis Conference, Orlando, Florida, Nov. 8-10, 1982.
19. Formenti, D., Richardson, M., "Parameter Estimation from Frequency Response Measurements Using Rational Fraction Polynomials (20 Years Of Progress)," Proceedings of the 20th International Modal Analysis Conference, Orlando, Florida, January 2002.
 20. Vold, H., "Numerically Robust Frequency Domain Modal Parameter Estimation," *Sound and Vibration*, January 1990.
 21. Vold, H., "Statistics of the Characteristic Polynomial in Modal Analysis," Proceedings of the 15th International Seminar on Modal Analysis, University of Leuven, September 1990.
 22. Rolain, Y., Pintelon, R., Xu, K. Q., and Vold, H., "On the Use of Orthogonal Polynomials in High-Order Frequency Domain System Identification and Its Application to Modal Parameter Estimation," Proceedings of the 33rd IEEE Conf Decis. Contr., Orlando, Florida, pp. 3365-3373, Dec. 14-16, 1994.
 23. Xu, K. Q., Rolain, Y., Vold, H., "High-Order Model Building in Frequency Domain Modal Analysis," 13th International Modal Analysis Conference, Nashville, Tennessee, February 1995.
 24. Rolain, Y., Pintelon, R., Xu, Q., Vold, H., "Best Conditioned Parametric Identification of Transfer Function Models in the Frequency Domain," *IEEE Transactions On Automatic Control*, Vol. 40, No. 11, November 1995.
 25. Vold, H., "Methods and Apparatus for Modal Parameter Estimation," Patent Application, filed June 26, 2006

Bibliography

1. Brincker, R., and Andersen, P., "Method for Vibration Analysis," United States Patent 6,779,404, August 24, 2004.
2. Moeller, N, Brincker, R., Herlufsen, H., and Andersen, P., "Modal Testing of Mechanical Structures Subject to Operational Excitation Forces," Proceedings of the 19th IMAC, 2001.
3. Vold, H., Crowley, J. R., Rocklin, G. T., "New Ways of Estimating Frequency Response Functions," *Sound and Vibration*, November 1984.
4. Vold, H., Leuridan, J., "High-Resolution Order Tracking at Extreme Slew Rates, using Kalman Tracking Filters," SAE Technical Paper No. 931288, Noise & Vibration Conference & Exposition, Traverse City, Michigan, May 1993.
5. Williams, R., Crowley, J. R., Vold, H., "The Multivariate Modal Indicator Function in Modal Analysis," Third International Modal Analysis Conference, January 1985. 

The author may be reached at: havard.vold@ata-e.com.